

Vibrational excitation functions for inelastic and superelastic electron scattering from the ground-electronic state in hot CO₂

H. Kato^a, H. Kawahara^a, M. Hoshino^a, H. Tanaka^a, L. Campbell^b, M.J. Brunger^{b,*}

^aDepartment of Physics, Sophia University, Chiyoda-ku, Tokyo 102-8554, Japan

^bARC Centre for Antimatter-Matter Studies, SoCPES, Flinders University, GPO Box 2100, Adelaide, SA 5001, Australia

ARTICLE INFO

Article history:

Received 4 August 2008

In final form 25 September 2008

Available online 1 October 2008

ABSTRACT

We report inelastic and superelastic excitation function measurements for electron scattering from the ground vibrational quantum (000), the bending vibrational quantum (010) and the unresolved first bending overtone (020) and symmetric stretch (100) modes of the ground-electronic state in hot (700 K) carbon dioxide (CO₂) molecules. The incident electron energy range of these measurements was 1–9 eV, with the relevant excitation functions being measured at the respective electron scattering angles of 30°, 60°, 90° and 120°. Where possible comparison is made to the often quite limited earlier data, with satisfactory agreement typically being found to within the cited experimental errors.

© 2008 Elsevier B.V. All rights reserved.

1. Introduction

While there have been several investigations, both experimental [1–4] and theoretical [5–7] (and references therein), into electron impact excitation of room temperature CO₂, where the predominant scattering occurs from the ground vibrational quantum (000) of the ground-electronic state (¹Σ_g⁺), studies into electron scattering from hot CO₂ are still quite limited. We believe that the first quantitative experiment to study low-energy electron scattering from vibrationally excited CO₂ molecules was by Buckman et al. [8], in which total cross sections (TCSs) as a function of temperature were determined using a linear attenuation time-of-flight (TOF) spectrometer. In that work Buckman et al. observed a substantial increase in the TCS at electron energies below 2 eV, which they attributed to enhanced scattering due to the electric dipole moment of the bending (010) mode. No significant change in the TCS was observed at higher energies. Ferch et al. [9] repeated the experiment of Buckman et al., also using a TOF spectrometer, and confirmed the earlier result of direct dipole scattering but also found, in contrast, a pronounced change (increase) in the TCS at energies from about 3 to 5 eV, where the ²Π_u resonant state of CO₂ is formed. The resonance contribution from the vibrationally excited (hot) molecules, again mainly in the (010) mode, was also observed to shift to lower energies, compared to the ground-state case, by about 0.3 eV. This point is important and is used later in our analysis. More recently, Strakeljahn et al. [10] confirmed the results from Ferch et al.

With respect to angular distribution measurements for electron scattering from hot CO₂, we are aware of only the data from John-

stone et al. [11], at an impact energy of 4 eV and scattering angle of 30°, and the somewhat more extensive results from Johnstone et al. [12], now at 3.8 eV but for the scattered electron angles 20°, 30°, 40°, 60° and 80°. These latter results obtained the first inelastic cross sections for scattering from the (010)^{*1} → (020)(100) modes and for superelastic scattering of the (010)^{*} mode to the ground-state (000) level. Nonetheless the available data in the literature remains quite limited. Indeed part of the rationale for the present study was to try to significantly extend the superelastic and inelastic vibrational cross sections that are available. This is not only important for providing benchmark data against which sophisticated theoretical calculations can be compared, but is also vital when trying to study the role of electron-driven processes on Venus and Mars where CO₂ is one of the two dominant atmospheric species [13].

In the next section of this Letter we describe our apparatus, measurement procedure and analysis techniques. Thereafter, in Section 3, are presented our results and a discussion of these results. Finally, some conclusions from this investigation are provided in Section 4.

2. Experimental and analysis details

The electron scattering apparatus has been described many times previously [1], and as a consequence we do not repeat all those details again here. Briefly, however, electrons from a 180° spherical monochromator intercept an effusive molecular beam of hot CO₂ by employing a crossed-beam system. Scattered electrons are subsequently energy analyzed in a second 180° spherical system. In order to reduce possible variations of the electron-beam

* Corresponding author. Fax: +618 8 82012905.

E-mail address: michael.brunger@flinders.edu.au (M.J. Brunger).

¹ * Indicates scattering from an excited vibrational mode of the CO₂ molecule.

current with different gases, all of the electron spectrometer is enclosed in separate casings and pumped differentially. The present vibrational excitation function experiments were performed with an overall energy resolution of about 30 meV, and with an incident current of the order of a few nA in the impact-energy range from 1 eV to 9 eV. The entire electron optics have been designed by beam tracing methods and they use computer controlled voltages which follow the energy sweeps, in order to keep the transmission constant. As noted later in this section the absolute scale has been placed by the relative flow method, corrected further for the effect of the target gas temperature on the gas flux by using $J \propto P/\sqrt{T}$, where J is the gas flux, P the target gas pressure and T the temperature of the target gas. The impact-energy scale was calibrated against the He resonance at 19.367 eV, as well as the $^2\Pi_g$ resonance of N_2 ($v = 1$) at 0.97 eV [14]. We believe this is accurate to ± 10 meV.

The CO_2 gas is heated using a cylindrical cell made of solid Cu, which incorporates a 4 mm long nozzle of 0.6 mm diameter. The cell itself has an internal diameter of 10 mm and a length of 12 mm, with a quartz fibre. The cell is heated by wrapping a resistive coaxial sheath wire around it, and can reach temperatures up to about 850 K. A magnetic shield, placed around the cell, prevents the field generated by the heater, around which there is wrapped a water flowing pipe that can cool as an outer jacket, from penetrating into the interaction region. A thermocouple was set in a small hole on the cell, and can serve to monitor the cell temperature. From our previous experiment [15] to produce a gas phase C_{60} beam, it has been confirmed that the gas temperature of the cell can be estimated approximately to be the same as that for the CO_2 beam at the collision centre (~ 1.5 – 2 mm from the cell nozzle exit).

A typical energy loss (gain) spectrum, taken at 700 K with an incident electron energy of 3.5 eV and a scattered electron angle of 90° , is shown in Fig. 1. As can be seen the peaks labelled 1 and 2 are both quite well-resolved from the elastic peak which, given our energy resolution of ~ 30 meV and the vibrational spectroscopy of CO_2 as summarised in Table 1, is the anticipated result. Peak 1 contains superelastic contributions from the $(010)^*-(000)$ and $(020)^*(100)^*-(010)^*$ transitions, while peak 2 originates from the inelastic $(000)-(010)$ and $(010)^*-(020)(100)$ transitions. The fact that these respective transitions in peaks 1 and 2 are not immediately resolvable in our energy loss (gain) spectra, owes a lot to the very harmonic nature of the vibrational modes in CO_2 (see Table 1). The experimental procedure is therefore as follows. The energy gain (loss) is set on the appropriate value for either peak 1 (2) and the number of true scattered counts is recorded on a multichannel analyser (MCA) as a function of incident electron energy (E_0), at a given electron scattering angle (θ). Great care must be taken during these measurements to ensure that no instrumental distortion of the measured (unresolved) excitation functions occur at each θ [16,17]. The absolute scale is now set using the relative flow technique [18] with helium and its well-established cross sections [19] as the standard gas. The result of this process is therefore, at each θ , an unresolved absolute excitation function for the $(010)^*-(000)+(020)^*(100)^*-(010)^*$ superelastic transitions and an unresolved absolute excitation function for the $(000)-(010)+(010)^*-(020)(100)$ inelastic transitions. In each case, we now attempt to uniquely deconvolve their respective contributions to peaks 1 and 2 by using the following assumptions in conjunction with a least squares fit [20] procedure:

- (1) In the deconvolution of peak 2 we, consistent with the results of Ferch et al. [9] and Strakeljahn et al. [10], insist that the maximum in the $(010)^*-(020)(100)$ excitation function occurs at an energy 0.3 eV lower than that for the $(000)-(010)$ excitation function.

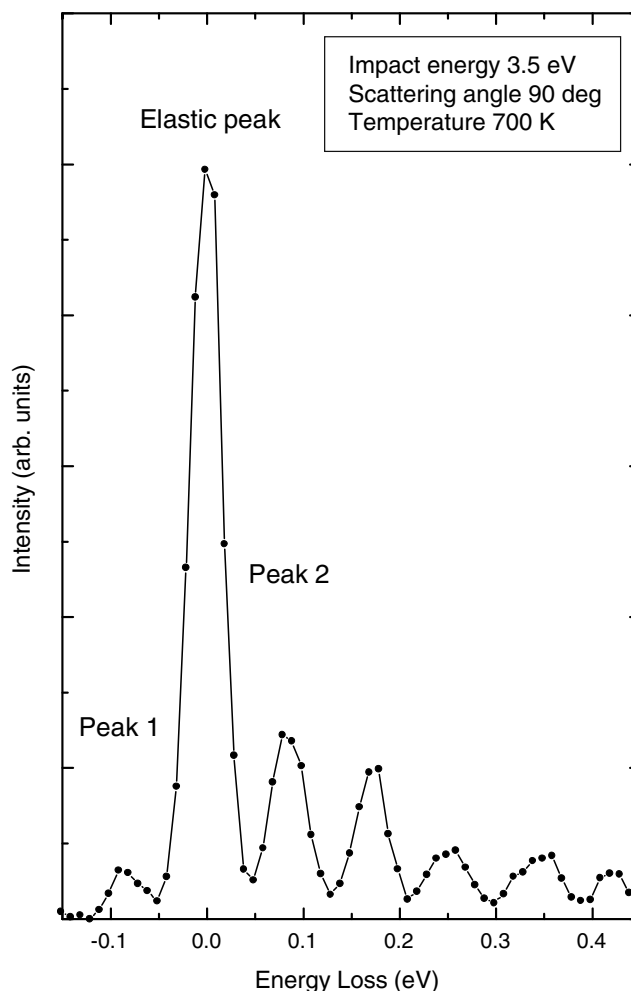


Fig. 1. Typical EELS spectrum of CO_2 at an impact energy of 3.5 eV and a scattering angle of 90° . The temperature of the CO_2 beam was 700 K.

Table 1

Population fractions, determined from a standard Boltzmann distribution [25], of the vibrational modes in the initial electronic-state of CO_2

Vibrational mode	Energy (meV)	Population fractions (%)		
		300 K	550 K	750 K
(000)	0.00	91.8632	66.4394	49.8724
(01 ¹ 0)	82.75	7.4819	23.1840	27.7222
(02 ⁰ 0)	159.37	0.1931	2.3018	4.2357
(02 ² 0)	165.54	0.3042	4.0416	7.7001
(10 ⁰ 0)	172.11	0.1180	1.7592	3.4779
(03 ¹ 0)	239.59	0.0173	0.8472	2.4485
(03 ³ 0)	248.38	0.0123	0.7038	2.1371
(11 ¹ 0)	257.50	0.0087	0.5806	1.8558
(00 ⁰ 1)	291.26	0.0012	0.1424	0.5504

The energies of the respective modes are taken from Ref. [12].

- (2) In the deconvolution of both peaks 1 and 2, in all relevant cases, we assume that the Principle of Detailed Balance (Fowler [21]) holds. For instance, in the case of the bending mode this means that the condition:

$$g_0 \sigma_{01}(E_0, \theta) = g_1 \sigma_{10}(E_0 - \Delta E_v, \theta) \quad (1)$$

must be maintained in the deconvolution process. Note that in Eq. (1) above g is the degeneracy, ΔE_v is the energy of the vibrational quantum excited, σ_{01} is shorthand notation for

the inelastic cross section for the (000)–(010) transition, while σ_{10} denotes the superelastic cross section for the (010)*–(000) transition. Further note that Johnstone et al. [12] looked at the validity of the Principle of Detailed Balance in their study, and found that it held to within their experimental uncertainty. We thus believe it is also reasonable to apply it in our analysis.

In Figs. 2 and 3 we therefore show the absolute excitation function results from this process, at each measured $\theta = 30^\circ, 60^\circ, 90^\circ,$ and 120° , for the (000)–(010), (010)*–(020)(100), (010)*–(000) and (020)*–(100)*–(010)* transitions. The overall errors on these excitation functions are in the range 20–70% and include contributions from the statistical accuracy of the data, an uncertainty in our experimental calibration procedures including our normalisation to set the absolute scale, and an uncertainty reflecting the uniqueness of our least squares fit deconvolutions. In the latter case this uncertainty is greater for the deconvolution of peak 1 vis-à-vis peak 2, as there are less constraints on the fitting of the components in peak 1.

Where possible, the present excitation functions are compared and discussed against corresponding earlier results in the next section. Here we simply highlight that as the method of Johnstone et al. [12], in deriving their cross sections, was very different to the present, such a comparison affords a potentially valuable cross check for both the present and earlier approaches employed.

3. Results and discussion

It is clear from Figs. 2 and 3 that the $^2\Pi_u$ resonance plays a significant role in enhancing the measured cross sections for all the excitation functions measured as a part of this study. It is also clear that there are no detailed theoretical calculations against which we can compare the present excitation functions. The only exception to this is the work of Takekawa and Itikawa [7] for the (000)–(010) transition. However, as that work predicts the resonance peak to occur at an energy ~ 1.2 eV higher than the accepted value, we do not plot its results here. It would for instance be particularly interesting if McCurdy et al. [6] were to extend their very sophisticated calculations for the Fermi dyad, to the present transitions. Having made these general observations, we now frame the discussion that follows by considering each of the inelastic and superelastic transitions in turn.

Let us begin our discussion by considering the relatively well-studied (000)–(010) inelastic transition, with the present excitation functions at 30° and 60° being given in Fig. 2a and b and our excitation functions at 90° and 120° being found in Fig. 3a and b. Also plotted in these figures, where possible, are earlier data from Antoni et al. [22], Register et al. [23] and Johnstone et al. [12]. Note that to ensure these plots did not get ‘too busy’, the previous results for (000)–(010) from our group [1] are not plotted on these figures. Further note that the cross sections (elastic, inelastic and superelastic) plotted in Fig. 3 of Johnstone et al. [12] were put on

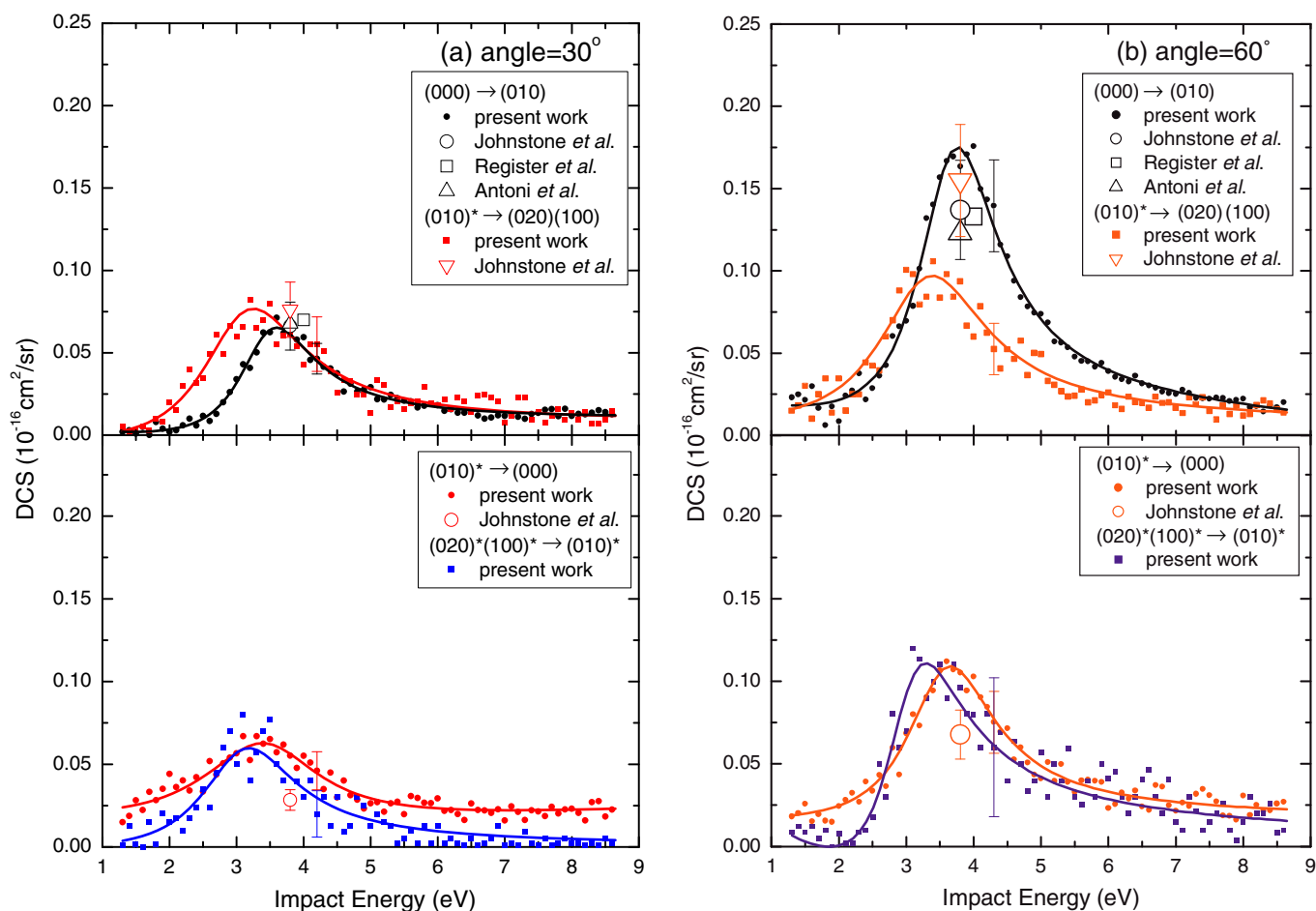


Fig. 2. Vibrational excitation functions for the inelastic (000) → (010) and (010)* → (020)(100) transitions and (010)* → (000) and (020)*–(100)* → (010)* superelastic transitions of CO₂ at impact energies of 1–9 eV and at scattering angles of (a) 30° and (b) 60°. In each case the solid line simply serves to highlight the observed energy dependence. See also legend for further details.

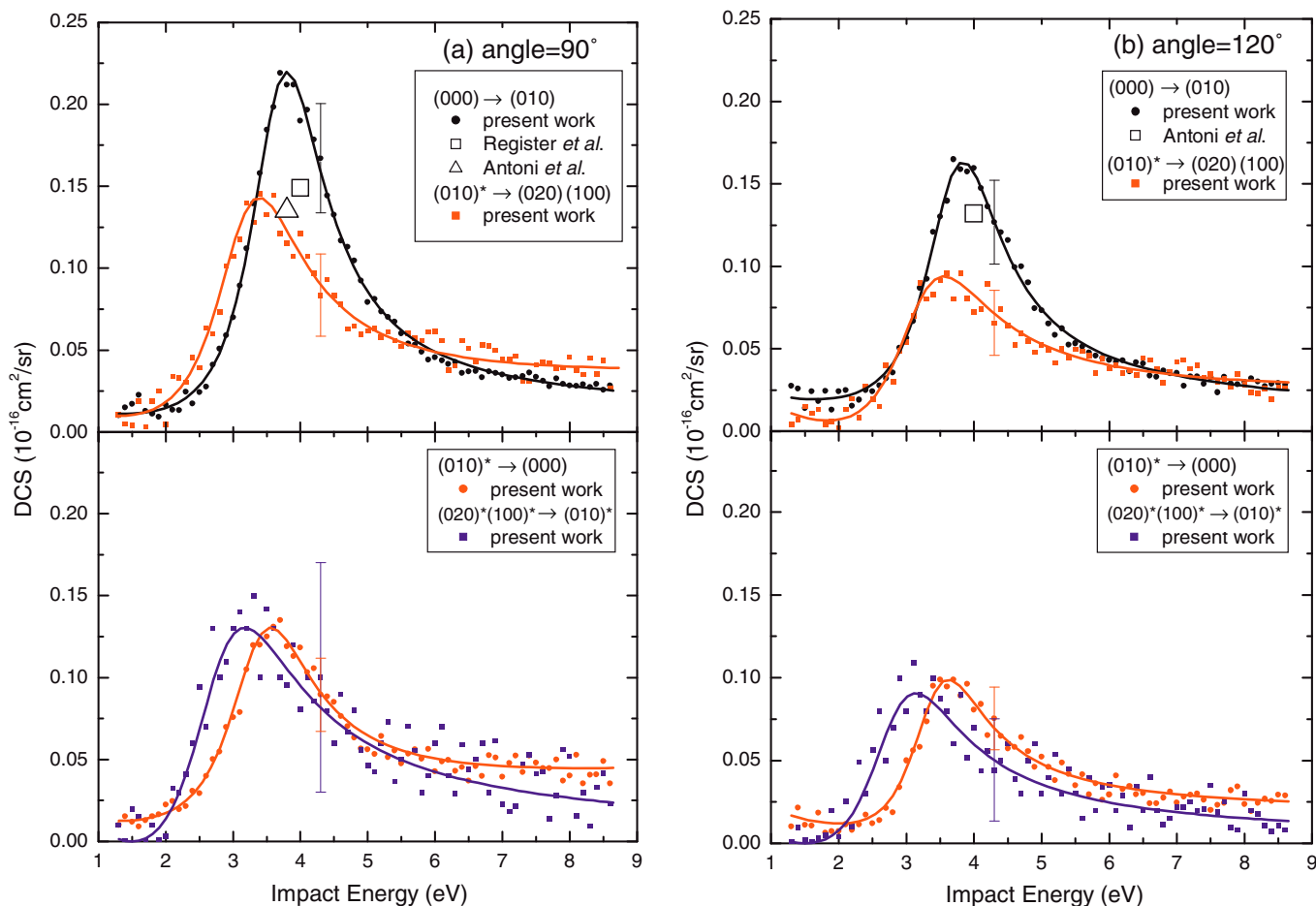


Fig. 3. Vibrational excitation functions for the inelastic $(000) \rightarrow (010)$ and $(010)^* \rightarrow (020)(100)$ transitions and $(010)^* \rightarrow (000)$ and $(020)^*(100)^* \rightarrow (010)^*$ superelastic transitions of CO_2 at impact energies of 1–9 eV and at scattering angles of (a) 90° and (b) 120° . In each case the solid line simply serves to highlight the observed energy dependence. See also legend for further details.

an absolute scale by using the elastic CO_2 data from Gibson et al. [24]. This applies to all the excitation functions we discuss in this section, not just for the (000) – (010) case. Finally we note that the uncertainty on the present (000) – (010) excitation functions are typically $\sim 20\%$. Considering Figs. 2 and 3 in more detail, then it is apparent that irrespective of the scattering angle good agreement, to within the cited uncertainties, is found between the present (000) – (010) excitation functions and the (010) differential cross section data taken from the earlier measurements [12,22,23]. Although not shown, the present (000) – (010) excitation function is also in excellent accord with the corresponding results from Kitajima et al. [1]. Together these observations give us confidence in both the apparatus calibration procedures we adopted for the current work and in the spectral deconvolutions of peak 2 in Fig. 1 that we performed.

The second inelastic transition we can consider is for the process $(010)^* \rightarrow (020)(100)$. Such an excitation function measurement is only possible here because (see Table 1) at 750 K the hot CO_2 beam consists of about 28% in the $(010)^*$ state. Note that in this case the uncertainty on the present $(010)^* \rightarrow (020)(100)$ data in Figs. 2 and 3 is typically $\sim 30\%$. Further note that here only a very limited comparison can be made between our results and those from Johnstone et al. [12] at one energy and for the scattering angles 30° and 60° . At 30° the datum point of Johnstone et al. is in very good agreement with the present result, however, at 60° the Johnstone et al. cross section is somewhat larger than the current one. Nonetheless when the error bars on the respective mea-

surements are taken into account we would characterise the overall level of agreement between them at 60° to be quite fair, with their error bars certainly overlapping.

We now examine our results for the superelastic scattering processes considered in this investigation, initially starting with the excitation function for the $(010)^* \rightarrow (000)$ process. Again we are limited in our discussion here to comparing against the earlier results from Johnstone et al. [12] at 30° and 60° . In this case the data from Johnstone et al., at both 30° and 60° , are found to have somewhat smaller cross sections than those determined from the present study. Nonetheless, similar to the inelastic case just described, the error bars on both sets of data would still overlap in each case, so that the overall level of agreement between ourselves and Johnstone et al. for the $(010)^* \rightarrow (000)$ transition is fair. We believe this is an important result, as we now have two processes ($(010)^* \rightarrow (020)(100)$ and $(010)^* \rightarrow (000)$) for which the cross sections determined in two rather different approaches are largely consistent. This gives us further confidence in the validity of both the present data and that from Johnstone et al. [12] for those transitions. Note that the typical uncertainty on our $(010)^* \rightarrow (000)$ excitation functions is $\sim 25\%$. Considering Figs. 2 and 3 in more detail, specifically concentrating on the magnitude of the cross sections at each θ at the resonance peak, we find that our cross section maxima increase steadily in value up to $\theta = 90^\circ$ and thereafter falls off again. For a ${}^2\Pi_u$ resonance in a linear molecule, with $\ell = 1$ being the strongest partial wave, at first glance this behaviour might naively appear to be a little anomalous (as $P_1(\cos\theta) = \cos(\theta) = 0$ at

$\theta = 90^\circ$). However, as McCurdy et al. [6] noted, upon bending the ${}^2\Pi_u$ resonance splits into two non-degenerate components of 2A_1 and 2B_1 symmetry, so that the angular dependence of the cross section (see Eq. (45) in McCurdy et al.) depends on some amplitude terms weighted by a $\cos 2\theta$ dependence. Hence the terms at $\theta = 90^\circ$ do not vanish in the more complete model when CO_2 bending is accounted for, and thus our observed angular dependence of the cross section maxima in the $(010)^*-(000)$ superelastic transition is not in fact anomalous.

The final superelastic process we consider in this study is for the $(020)^*(100)^*-(010)^*$ transition. In this case the data is original, there having been no other measurements for its cross sections. Note that our typical estimated uncertainty on the excitation functions in Figs. 2 and 3 is $\sim 70\%$ for this process, at least in part reflecting the fact that even at 750 K the unresolved (02^00) , (02^20) and (100) modes constitute only $\sim 15\%$ (see Table 1) of the hot CO_2 beam. It is clear from Figs. 2 and 3 that all the excitation functions for the $(020)^*(100)^*-(010)^*$ process have the same qualitative energy dependence as those already discussed, although the scatter in the measured data is much more prevalent in this case.

4. Conclusions

We have reported absolute excitation functions for the $(000)-(010)$ and $(010)^*-(020)(100)$ inelastic and $(010)^*-(000)$ and $(020)^*(100)^*-(010)^*$ superelastic transitions for electron scattering from hot CO_2 . To accomplish this a novel deconvolution procedure was applied to the measured energy loss/gain spectra, at each of the electron scattering angles 30° , 60° , 90° and 120° . This procedure, involving a 0.3 eV shift in the resonance peak of the excitation functions to lower energies where appropriate and applying the principle of detailed balance, suggests a new methodology to determine reliable cross sections for scattering from vibrationally excited species. We note that the present excitation functions significantly extend our knowledge of the cross sections for the above processes. Where a comparison with previous data was possible generally fair agreement was found to within the measurement uncertainties, thereby giving us confidence in both our instrumental calibration procedures and in the validity of the data we have reported. We hope that the present measurements will now stimulate theory to investigate the processes we have studied in more detail, with only the calculation from Takekawa and Itikawa [7] for the inelastic $(000)-(010)$ excitation currently being known to us. Finally we believe that the branching ratio between the resonant vibrational excitation cross sections for ground-state and hot CO_2

scattering, which are the most effective processes for the thermalisation of lower energy electrons, provides important information for the modelling of upper atmospheric phenomena.

Acknowledgements

This work was conducted at Sophia University under the auspices of the Japanese Ministry of Education, Sport, Culture and Technology. One of us (H. Kato) acknowledges the Japan Society for the Promotion of Science (JSPS) for his fellowship as a grant-in-aid for scientific research. L.C. and M.J.B. thank the ARC Centre for Antimatter-Matter Studies for some additional financial support. We all thank the International Atomic Energy Agency (IAEA) for its support of this work as a part of a data base project.

References

- [1] M. Kitajima, S. Watanabe, H. Tanaka, M. Takekawa, M. Kimura, Y. Itikawa, *J. Phys. B* 34 (2001) 1929.
- [2] M. Allan, *Phys. Rev. Lett.* 87 (2001) 033201.
- [3] M. Allan, *J. Phys. B* 35 (2002) L387.
- [4] M.J. Brunger, S.J. Buckman, M.T. Elford, in: Y. Itikawa (Ed.), *Photon and Electron Interactions with Atoms Molecules and Ions*, Landolt-Börnstein, vol. 1/17C, Springer, New York, 2003.
- [5] M.A. Morrison, A.E. Greene, *J. Geophys. Res.* 83 (1978) 1172.
- [6] C.W. McCurdy, W.A. Isaacs, H.-D. Meyer, T.N. Rescigno, *Phys. Rev. A* 67 (2003) 042708.
- [7] M. Takekawa, Y. Itikawa, *J. Phys. B* 32 (1999) 4209.
- [8] S.J. Buckman, M.T. Elford, D.S. Newman, *J. Phys. B* 20 (1987) 5175.
- [9] J. Ferch, C. Masche, W. Raith, L. Wiemann, *Phys. Rev. A* 40 (1989) 5407.
- [10] G. Strakeljahn, J. Ferch, W. Raith, in: J.B.A. Mitchell, J.W. McConkey, C.E. Brion (Eds.), *Proc. 19th ICPEAC*, British Columbia University Press, Whistler, 1995, p. 428.
- [11] W.M. Johnstone, N.J. Mason, W.R. Newell, *J. Phys. B* 26 (1993) L147.
- [12] W.M. Johnstone, M.J. Brunger, W.R. Newell, *J. Phys. B* 32 (1999) 5779.
- [13] L. Campbell, M.J. Brunger, T.N. Rescigno, *J. Geophys. Res.* 113 (2008) E08008, doi:10.1029/2008JE003099.
- [14] W. Sun et al., *Phys. Rev. A* 52 (1995) 1229.
- [15] H. Tanaka, L. Boesten, K. Onda, O. Ohashi, *J. Phys. Soc. Jpn.* 63 (1994) 485.
- [16] M.J. Brunger, S.J. Buckman, *Phys. Rep.* 357 (2002) 215.
- [17] M. Allan, *J. Phys. B* 38 (2005) 3655.
- [18] J.C. Nickel, P.W. Zetner, G. Shen, S. Trajmar, *J. Phys. E* 22 (1989) 730.
- [19] L. Boesten, H. Tanaka, *Atom Data Nucl. Data Tables* 52 (1992) 2.
- [20] P.R. Bevington, D.K. Robinson, *Data Reduction and Error Analysis in the Physical Sciences*, Mc Graw-Hill, New York, 1990.
- [21] R.H. Fowler, *Statistical Mechanics: The Theory of the Properties of Matter in Equilibrium*, The University Press, Cambridge, 1936.
- [22] Th. Antoni, K. Jung, H. Ehrhardt, E. Chang, *J. Phys. B* 19 (1986) 1377.
- [23] D.F. Register, H. Nishimura, S. Trajmar, *J. Phys. B* 13 (1980) 1651.
- [24] J.C. Gibson, M.A. Green, K.W. Trantham, S.J. Buckman, P.J.O. Teubner, M.J. Brunger, *J. Phys. B* 32 (1999) 213.
- [25] G. Herzberg, *Molecular Spectra and Molecular Structure*, vol. 2, *Infra Red and Raman Spectra of Polyatomic Molecules*, van Nostrand, New York, 1945.